XLI CILAMCE
XLI Ibero-Latin American Congress on Computational Methods in Engineering
16-19 November, 2020 FOZ DO IGUAÇU PARANÁ - BRAZIL

Virtual element method: who are the virtual functions?

Tiago Fernandes Moherdaui[1], Alfredo Gay Neto[2]

[1]*Dept. of Structural and Geotechnical Engineering, University of São Paulo*
Av. Prof. Almeida Prado, 83, 05508-070, São Paulo, Brazil
tiago.moherdaui@usp.br
[2]*Dept. of Structural and Geotechnical Engineering, University of São Paulo*
Av. Prof. Almeida Prado, 83, 05508-070, São Paulo, Brazil
alfredo.gay@usp.br

Abstract. The Virtual Element Method (VEM) is a generalization of the Finite Element Method (FEM). It proposes approximations to fields of interest on elements of almost any shape, by employing a function space containing a full polynomial space of arbitrary degree, for its convergence properties, along with additional suitable functions. The degrees of freedom of the element are designed such that these additional functions can remain unknown while solving the discretized version of the problem. A term containing the projection of the approximate solution onto the polynomial functions space guarantees the method's consistency, while a term with projection's residual has to be approximated to ensure stability. The approximation for the latter term is still an open problem for many applications. The objective of this paper is to show a procedure to solve for these virtual functions, their projection onto the polynomial space and its residual. This is proposed for the 2D Poisson problem, by presenting the functions as solutions, and solving for them via FEM. Then, finding their polynomial projection and the residual of the projection. From this, the stabilization term can be approximated up to the error of the FEM solution. This procedure may be a clue to visualize the virtual functions behavior and, in future, to help on proposing stabilization schemes.

Keywords: Virtual Element Method, Virtual Functions, Finite Element Method.

1 Introduction

The virtual element method was first introduced in Beirão da Veiga, et al. [1], and can be described as a generalization of the finite element method. One of the method's main advantages is the decoupling of element geometry from the polynomial space of functions used in the element-wise interpolation. The method uses a function space designed to include an arbitrary full polynomial space, in order to retain the convergence properties from the equivalent finite element.

This geometric versatility has inspired new strategies for problems in which changes in the mesh are useful/required. To mention a couple of examples: an excellent work in brittle material crack-propagation exploring VEM's characteristics was developed in Hussein, et al. [2]; and a new approach to contact modeling using the node-to-node formulation via clever use of node insertion was presented in Wriggers, Rust and Reddy [3].

The method consists of constructing an approximation space defined by a set of properties that encompass the full polynomial space, plus other (possibly) non-polynomial functions. Through careful choice of degrees of freedom, the appropriate matrices (stiffness matrix, mass matrix, etc.) can be computed without knowledge of these additional functions. Due to that the method is qualified as "virtual", since the full approximation space is usually not completely known.

Advantage comes at a cost. For the computations to be possible, the basis functions for this space must be split into their polynomial projection and a residual. The stiffness matrix encompasses two terms, one being a product of projections, and the other of residuals. The first term guarantees the methods consistency, and

the second its stability. This stability term must be approximated, as the functions are unknown. These approximations are currently an open problem. Some works regarding this are: Beirão da Veiga, Lovadina and Russo [4] overview of the method's stabilization; Wriggers, Rust and Reddy [3] with a specific stabilization for the proposed contact method, taking into account the presence of smaller colinear edges due to node insertion; a stabilization strategy for nonlinear hyperelasticity by introducing a new term in the problem's potential is introduced in Wriggers, et al. [5]; a similar approach in van Huyssteen and Reddy [6]. The objective of this paper is to propose a procedure to solve for these virtual functions for the 2D Poisson problem, evaluating their polynomial projection and residual using the FEM. As well as computing the stabilization term up to FEM's approximation error. This may be a clue to visualize the virtual functions behavior and, in future, to help on proposing stabilization schemes. This was motivated by an earlier work, Moherdaui and Gay Neto [7] , applying the method for a problem of this same type,
In section 2 the virtual element method is presented in the context of the 2D Poisson problem. In section 3 the methodology is explained. Sections 4 and 5 have the results and conclusions.

2 Virtual element method

The virtual element method consists of a procedure to generate a finite dimensional subspace of the space in which the weak solution of the problem resides. For the presentation of the method, the 2D Poisson problem is chosen to provide context, as it is used in the introductory papers for the method, as well as is used to obtain the virtual functions, as will be further explored in section 3.1.
The 2D Poisson problem is stated in its differential form as finding the function $u \in C^2(\Omega)$ satisfying eq.(1), where u: $\mathbb{R}^2 \supset \Omega \rightarrow \mathbb{R}$, and $\partial\Omega$ is the boundary of the domain (Ω) over which the problem is defined.

$$\begin{cases} \Delta u = -f \ in \ \Omega \\ u = \bar{u} \ in \ \partial\Omega \end{cases} \tag{1}$$

The same problem can be expressed in the weak formulation as finding the function $u \in H^1(\Omega)$ such that for any $\delta u \in H_0^1(\Omega)$ eq. (2) holds.

$$\begin{cases} \int_\Omega \nabla u \cdot \nabla \delta u \, d\Omega = \int_\Omega f \delta u \, d\Omega \\ u = \bar{u} \ in \ \partial\Omega \end{cases} \tag{2}$$

From the weak form, the requirement for the solution u is that is belongs to the infinite-dimensional Sobolev space H^1, i.e. itself and its first derivatives must be square integrable functions.

2.1 Discretization

The solution of the problem employing the VEM is attained via approximation of the exact solution in a constructed finite-dimensional space $V_k^h(\Omega)$, the global virtual function space, where k stands for the degree of the full polynomial space included. The discrete problem is stated as in eq. (2), only exchanging the exact solution and test function $u, \delta u \in H^1$ for their restricted counterparts $u_h, \delta u_h \in V_k^h \subset H^1$.
The global virtual function space is constructed based on a partition of the domain into subdomains Ω_e corresponding to the virtual elements. The union of the local virtual element spaces $V_k^h(\Omega_e)$ results in the global space. Each local space is comprised of all functions v_h that satisfy the properties stated below:

i. v_h is a polynomial of degree k on each edge e of Ω_e, i.e. $v_h|_e \in P_k(e)$;
ii. v_h on $\partial\Omega_e$ is globally continuous, i.e. $v_h|_{\Omega_e} \in C^0(\Omega_e)$;
iii. Δv_h is a polynomial of degree $k-2$ in Ω_e, i.e. $\Delta v_h \in P_{k-2}(\Omega_e)$.

For simplicity, a virtual element will be treated as a polygon with nv vertices and sides. The vertices are denoted by V and the sides (edges) by e, as shown in Figure 1. Other important quantities are the subdomain's measure $|\Omega_e|$, corresponding to its area, and its diameter h_e consisting of the largest distance between two points in the domain.
Introducing the discretization into the orthogonality condition leads to the linear system characterized by the stiffness matrix, the vector of degrees of freedom (DOFs) and the load vector. Each component in the stiffness

matrix is computed as shown in eq. (3). The functions denoted by ϕ are the canonical basis function for the DOFs that are stated later in this section. These functions are, for now, unknown.

$$(K^e)_{ij} = \int_{\Omega_e} \nabla\phi_i \cdot \nabla\phi_j \, d\Omega \tag{3}$$

A polynomial projection $\Pi_k^\nabla : V_k^h(\Omega_e) \to P_k(\Omega_e)$ is used to split the stiffness matrix into two terms, by applying it to both basis functions in eq. (3), as shown in eq. (4). The first integral corresponds to the consistency term (K_c^e), and the second term to the stability term (K_s^e). In the equation below ($I - \Pi_k^\nabla$) is the projector to the residual of the polynomial projection.

$$(K^e)_{ij} = \int_{\Omega_e} \nabla(\Pi_k^\nabla\phi_i) \cdot \nabla(\Pi_k^\nabla\phi_j) \, d\Omega + \int_{\Omega_e} \nabla((\mathrm{I} - \Pi_k^\nabla)\phi_i) \cdot \nabla((\mathrm{I} - \Pi_k^\nabla)\phi_j) \, d\Omega \tag{4}$$

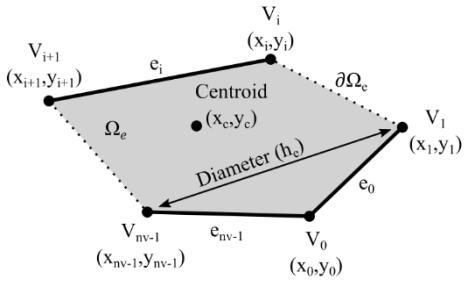

Figure 1. Generic virtual element.

The polynomial projection is based on the same orthogonality condition and is defined in eq. (5) below. This defines the projection up to a constant, there is an additional projector used to circumvent this kernel which is presented in Beirão da Veiga, et al. [8].

$$\int_{\Omega_e} \nabla p \cdot \nabla((\mathrm{I} - \Pi_k^\nabla)v_h) \, d\Omega = 0, \forall \, p \in P_k(\Omega_e) \tag{5}$$

The matrix form of this projector requires the computation of integrals involving virtual functions, of the type shown in the left-hand side of eq. (6). On the right-hand side is the form that relates to the degrees of freedom, where $\boldsymbol{n}$ is the exterior normal on the boundary. We'll chose a specific basis for the polynomial space called the scaled monomials (m_α). These are monomials centered on the element centroid and scaled by the inverse of the element's diameter. This is presented more in depth in Beirão da Veiga, et al. [8].

$$\int_{\Omega_e} \nabla m_\alpha \cdot \nabla v_h \, d\Omega = \int_{\partial\Omega_e} (\nabla m_\alpha \cdot \boldsymbol{n}) v_h \, d\partial\Omega - \int_{\Omega_e} \Delta m_\alpha v_h \, d\Omega_e \tag{6}$$

Finally, the degrees of freedom that univocally characterize a function v_h in the virtual function space are:

- The value of v_h at each of the nv vertices;
- The value of v_h at the $k-1$ internal points of the (k+1)-point Gauss-Lobatto quadrature on each edge;
- The moments up to order $k-2$ of v_h in Ω_e.

The moments referred to in the last set of DOFs are defined in eq. (7).

$$\frac{1}{|\Omega_e|} \int_{\Omega_e} v_h m_\alpha \, d\Omega, \alpha = 1, \dots, \dim(\mathrm{P}_{k-2}) \tag{7}$$

These degrees of freedom are enough to exactly compute the right-hand side of eq. (6). The boundary integral is solved exactly using the Gauss-Lobatto quadrature with the first two sets of DOFs, and the second integral corresponds to the third set. This fully accounts for the consistency term in eq. (4). Although the stability term's approximation is an open problem, for this particular problem the approximation presented in eq. (8) is sufficient, according to Beirão da Veiga, et al. [1]. The bold quantities refer to their matrix form based on the degrees of freedom stated earlier. The requirement for this approximation is that it scales in the same way

as the integral being approximated.

$$(\mathrm{K}_{\mathrm{s}}^{\mathrm{e}})_{\mathrm{ij}} = \int_{\Omega_e} \nabla((\mathrm{I} - \Pi_k^{\nabla})\phi_i) \cdot \nabla((\mathrm{I} - \Pi_k^{\nabla})\phi_j)\, d\Omega \approx \left(\mathbf{I} - \mathbf{\Pi}_{\mathbf{k}}^{\nabla}\right)\boldsymbol{\phi}_{\mathbf{i}} \cdot (\mathbf{I} - \mathbf{\Pi}_{\mathbf{k}}^{\nabla})\boldsymbol{\phi}_{\mathbf{j}} \tag{8}$$

The number of dimensions of a space $V_k^e(\Omega_e)$ can be explicitly calculated in terms of k and nv, as shown in eq. (9). The dimension of its polynomial subspace $P_k(\Omega_e)$ is stated, in terms of k, in eq. (10). And therefore, the dimension of their quotient space, the space of the residue, is obtained by taking the difference.

$$\dim V_k^e = nv + nv(k-1) + \dim P_{k-2} = nv * k + \frac{(k-1)k}{2} \tag{9}$$

$$\dim P_k = \frac{(k+1)(k+2)}{2} \tag{10}$$

For a more thorough and practical introduction to the method refer to Beirão da Veiga, et al. [8].

3 Methodology

This study of the virtual functions is done through the canonical basis functions for the degrees of freedom stated in the last section. In section 3.1 these will be shown to be solutions to Poisson problems, to be solved using the finite element method. Three different geometrical configurations are used, each with an associated mesh, as explained in section 3.2.

The polynomial approximations are obtained via linear combination of the scaled monomials, with weights obtained from the columns of the polynomial projector's matrix form. These are represented in the same mesh, and the residual is a matter of nodewise subtraction of the polynomial approximation from the basis function. Once the residuals are stored, the stability term can be computed exactly up to the finite element approximation. All visualizations were generated using the software GMSH by Geuzaine and Remacle [9].

3.1 Basis functions as Poisson-type problems

As shown at the beginning of section 2.1, the virtual functions are, by definition, globally continuous on the boundary of the element, and a polynomial of degree k on each edge. A unique polynomial of degree k on an edge is determined by its value at k+1 points. Therefore, the first and second set of DOFs fully determines its trace. These are used as Dirichlet boundary conditions for each basis functions.

Property (iii) requires the function's Laplacian to be a (k-2)-polynomial, this fits the definition of a Poisson problem shown in eq. (1). The exact polynomial is not known a priori, but the internal degree of freedom can be used to find the solution indirectly via linear combination of solutions of similar problems.

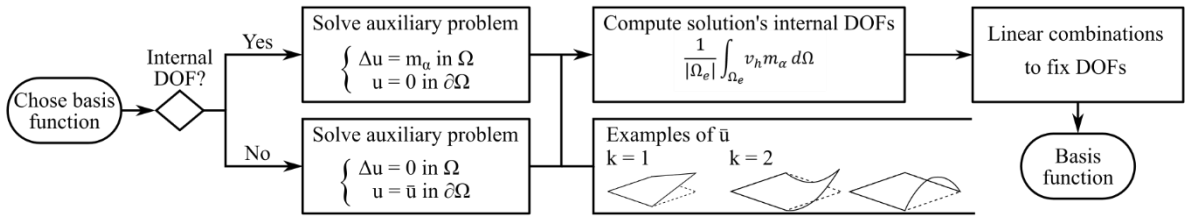

Figure 2. Procedure flowchart.

3.2 Chosen examples

The chosen examples to illustrate the results of this procedure consist of:

- Regular polygons (Triangle – T3, Square – S4), as most works using this method employ Voronoi-type meshes to showcase the method's geometrical versatility.
- Degenerate polygon (Quadrilateral – T4), meant as a Triangle with additional node on one side. This was chosen as some applications may take advantage of inserting new nodes, as is proposed in Wriggers, Rust and Reddy [3].

Although these examples are mostly restricted to usual polygons, the methodology presented to obtain those functions seems to be valid for any straight-sided shape, convex or not.
The geometries (shape and vertices) and meshes used are presented in Figure 3. The dimensions of the virtual space $V_k^e(\Omega_e)$, its polynomial subspace $P_k(\Omega_e)$ and the residual space V_k^e/P_k are presented in Table 1.

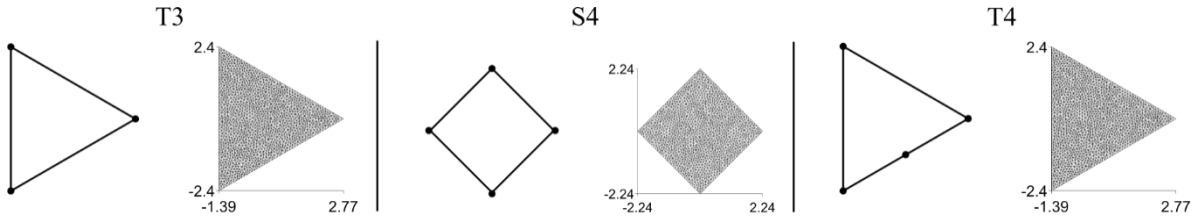

Figure 3. Selected examples: geometry (shape and vertices) and meshes.

Table 1. Dimensions of the function spaces in terms of polynomial degree and number of vertices.

	$\dim V_k^e$		$\dim V_k^e/P_k$		$\dim P_k$
k/nv	3	4	3	4	
1	3	4	0	1	3
2	7	9	1	3	6

4 Results

The results for T3, S4 and T4 are presented in Figure 4, Figure 5, and Figure 6, respectively. Taking advantage of symmetry for the regular polygons, the figures present the vertex basis functions for linear virtual element; for the quadratic case the basis functions are presented one of each: vertex, edge, and internal DOF. The basis function, polynomial projection and residual are presented together. For T4, the basis functions shown are those related to the additional node.
Table 1 shows that the virtual function space and space of linear polynomials coincide for the linear triangular element. This is evident in Figure 1 (a). For the quadratic function space, the residue consists of one dimension, this is shown as the residue of (c) and (d) are the same except for a scaling factor, and for (b) this scaling factor coincides with 0, as the virtual function coincides with the quadratic polynomial.

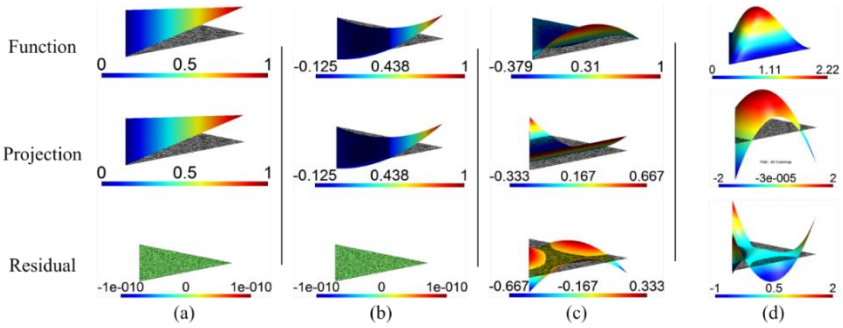

Figure 4. Basis functions, projection and residue for T3: (a) linear vertex DOF, quadratic (b) vertex, (c) edge, and (d) internal DOFs.

For the square geometry (S4), the linear function space has 1-dimensional residue, this is illustrated in Figure 5 (a), this residual is a second-order polynomial, and if the square were oriented with aligned with the axis it would correspond to the scaled analog to xy, which is normally added for linear quadrilateral finite elements. The quadratic functions induce a 3-dimensional residue space, this can be inferred by the clearly different symmetries in the residue functions presented: (b) is symmetric along the diagonal, (c) along the middle line

and (d) has two symmetries.

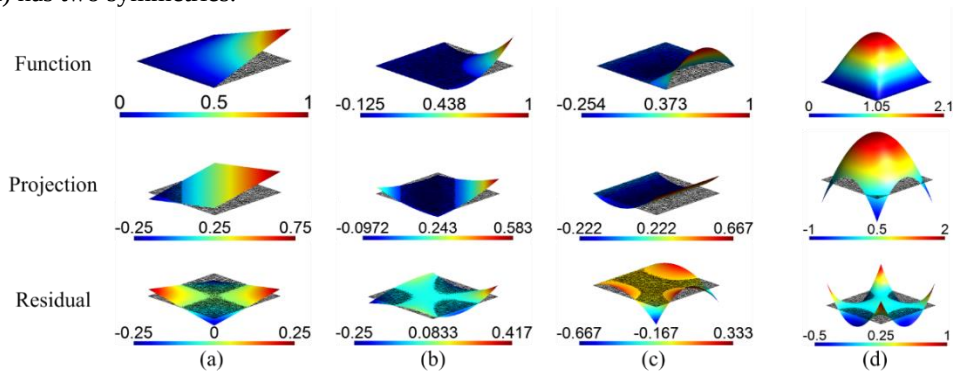

Figure 5. Basis functions, projection and residue for S4: (a) linear vertex DOF, quadratic (b) vertex, (c) edge, and (d) internal DOFs.

For the degenerated quadrilateral geometry (T4), the size of the residue space is the same as for the square, however the internal basis function is the same as for the triangle. There are points with slope discontinuity due to the nature of the basis functions and the colinear node.

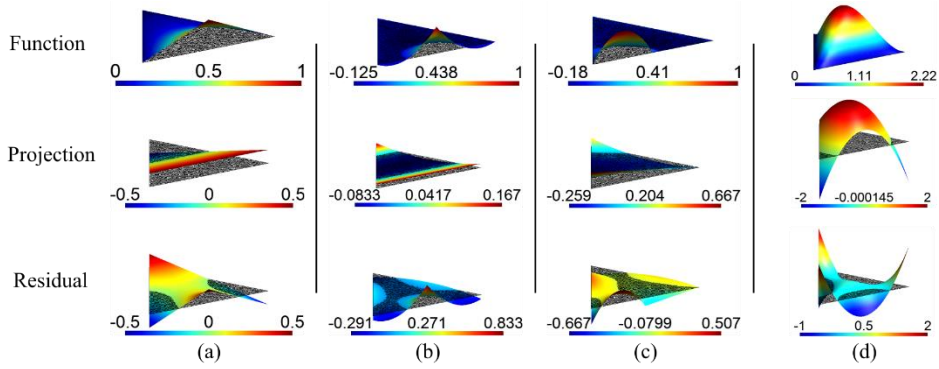

Figure 6. Basis functions, projection and residue for T4: (a) linear vertex DOF, quadratic (b) vertex, (c) edge, and (d) internal DOFs.

Figure 7 shows a comparison between the stiffness matrix stemming from FEM's approximation of the stability term for T3 and its approximation using eq. (8). The colors illustrate similar terms, showcasing the requirement that the approximation scales as the exact term does. The blocks of zeros correspond to the DOFs where the basis function coincide with a polynomial, leading to no residual.

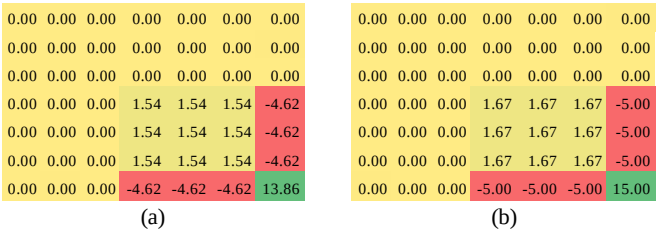

Figure 7. Stability stiffness matrix for quadratic T3 obtained via (a) FEM and (b) approximation.

Figure 8 show the same for the square configuration (S4). The same pattern is seen on both sides.

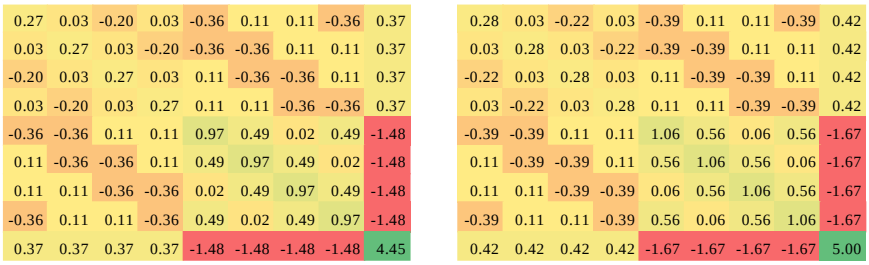

Figure 8. Stability stiffness matrix for quadratic S4 obtained via (a) FEM and (b) approximation.

5 Conclusions

The methodology was successful in obtaining the basis functions, their projection and residual, as well as being able to compute the stabilization term up to the FEM error. These same basis functions are used in other elliptic problems (e.g. elasticity). Using this procedure inside the actual method would be extremely impractical, however it might be useful for studying the exact stability term in the face of more complex problems. Although not shown, the presented procedure seems to be applicable for any straight-sided shape and polynomial order.
Another possible application for this is to inspire better post-processing and visualization tools for the results. Although the method's ingenuity is in not requiring knowledge of these functions, being familiar with them might be advantageous to better understand it and its results, such as to inspire the proposal of stabilization schemes.

Acknowledgements. The authors acknowledge Vale S.A. for the support through Wheel-Rail Chair project. The second author acknowledges CNPq (Conselho Nacional de Desenvolvimento Científico e Tecnológico) under the Grant 304680/2018-4.

Authorship statement. The authors hereby confirm that they are the sole liable persons responsible for the authorship of this work, and that all material that has been herein included as part of the present paper is either the property (and authorship) of the authors, or has the permission of the owners to be included here.

References

[1] L. Beirão da Veiga, F. Brezzi, A. Cangiani, G. Manzini, L. D. Marini, and A. Russo, "Basic Principles of Virtual Element Methods," *Math. Model. Methods Appl. Sci.*, vol. 23, no. 01, pp. 199–214, 2013, doi: 10.1142/S0218202512500492.

[2] A. Hussein, F. Aldakheel, B. Hudobivnik, P. Wriggers, P. A. Guidault, and O. Allix, "A computational framework for brittle crack-propagation based on efficient virtual element method," *Finite Elem. Anal. Des.*, vol. 159, no. March, pp. 15–32, 2019, doi: 10.1016/j.finel.2019.03.001.

[3] P. Wriggers, W. T. Rust, and B. D. Reddy, "A virtual element method for contact," *Comput. Mech.*, vol. 58, no. 6, pp. 1039–1050, 2016, doi: 10.1007/s00466-016-1331-x.

[4] L. Beirão da Veiga, C. Lovadina, and A. Russo, "Stability Analysis for the Virtual Element Method," 2016, doi: 10.1142/S021820251750052X.

[5] P. Wriggers, B. D. Reddy, W. Rust, and B. Hudobivnik, "Efficient virtual element formulations for compressible and incompressible finite deformations," *Comput. Mech.*, vol. 60, no. 2, pp. 253–268, 2017, doi: 10.1007/s00466-017-1405-4.

[6] D. van Huyssteen and B. D. Reddy, "A virtual element method for isotropic hyperelasticity," *Comput. Methods Appl. Mech. Eng.*, vol. 367, p. 113134, 2020, doi: 10.1016/j.cma.2020.113134.

[7] T. F. Moherdaui and A. Gay Neto, "Virtual Element Method vs Finite Element Method for Prandtl's Solution of St. Venant's Torsion Problem," in *Proceedings of the XL Ibero-Latin American Congress on Computational Methods in Engineering*, 2019.

[8] L. Beirão da Veiga, F. Brezzi, L. D. Marini, and A. Russo, "The Hitchhiker's Guide to the Virtual Element Method," *Math. Model. Methods Appl. Sci.*, vol. 24, no. 08, pp. 1541–1573, 2014, doi: 10.1142/S021820251440003X.

[9] C. Geuzaine and J.-F. Remacle, "A three-dimensional finite element mesh generator with built-in pre- and post-processing facilities," *Int. J. Numer. Meth. Engng.*, vol. 79, no. 11, pp. 1309–1331, 2017, [Online]. Available: http://gmsh.info/doc/preprints/gmsh_paper_preprint.pdf%0Ahttp://gmsh.info/.